Establishing the Correspondence Between Control Points in Pairs of Mammographic Images

Nenad Vujovic, *Student Member, IEEE,* and Dragana Brzakovic, *Member, IEEE*

***Abstract*— This paper describes part of a study aimed at developing a computer-based aid for mammogram screening that makes a detailed comparison between mammograms of the same patient acquired at different screenings and detects changes indicative of cancer. The focus is on determining control points in two mammograms; these points are used to put two mammograms into correspondence. The paper details the algorithm for identifying the potential control points and establishing the correspondence between the two sets of control points. The algorithm's performance was evaluated by three observers, one of whom is an experienced radiologist, and found to be adequate.**

***Index Terms*— Control points, correspondence, digital mammography, registration.**

I. Introduction

THERE IS strong evidence that early cancer detection is the key to successful treatment (from the functional and aesthetic points of view), low cost treatment, and reduction of mortality. Routine mammograms are recommended for a large percentage of the female population as the most reliable early detection method. Computer technology offers a means of improving the accuracy of mammogram readings while lowering the cost of the procedure—both improvements being necessary preconditions for the implementation of widespread screening programs. Many recent studies have attempted to develop a computer-based aid for mammographic screenings. Most of the proposed approaches consider a single mammogram and utilize complex image processing and/or pattern recognition methods to enhance or detect one of the two most common signs of cancer [1]: 1) abnormal regions of breast parenchyma, e.g., stellate lesions, and 2) microcalcifications. Research efforts in the first category concentrate on enhancing mammograms [2], [3] and detecting particular classes of tumors [4], [5]. The image processing techniques used by various researchers vary from calculating local statistics of a pixel neighborhood [6] to texture measurements [7] and estimating fractal dimension [8]. The studies concentrating on microcalcifications can be divided into detection [9], [10] and classification [11], [12].

Manuscript received December 24, 1995; revised January 20, 1997. This work was supported by the NSF under Grant IRI-9504363 and by the U.S. Army under Grant DAMD17–96–1–6128. The associate editor coordinating the review of this manuscript and approving it for publication was Dr. Maria Petrou.

The authors are with the Department of Electrical Engineering and Computer Science, Lehigh University, Bethlehem, PA 18015 USA (e-mail: db09@lehigh.edu).

Publisher Item Identifier S 1057-7149(97)07023-1.

The work described in this paper is motivated by the problem of automated mammogram followup, i.e., detection of abnormalities by comparing different screenings of the same patient. The major advantage of automated followup is that the abnormality is determined by using the older mammogram as a reference, and thus, the decision regarding presence of abnormalities is made in the context of particular patient's mammograms. Furthermore, automated followup has the potential to provide for very early cancer detection, possibly earlier than presently possible. However, the problem of automated mammogram followup is very complex and requires solving a number of subproblems, including standardizing screening procedures, registering mammograms, and characterizing minor changes in texture patterns. This paper focuses on the first step of mammogram registration, i.e., identification of control points in two mammograms that can be used in establishing regional correspondence between two images.

Mammograms are projections of compressed three-dimensional (3-D) structures, and their analysis requires relating the observed two-dimensional (2-D) structures to a feasible 3-D arrangement of tissue. Primary sources of misregistration are differences in 3-D positioning and compression, which manifest in visually different images. The problem of relating misregistration of 2-D images to a change in viewpoint and 3-D object appearance is commonly encountered in computer vision, e.g., stereo imaging. However, the problem at hand is considerably more complex because the 3-D object is elastic and subject to compression. The additional sources of difficulties include lack of clearly defined landmarks and normal variations in breast tissue over time. Strictly speaking, precise mammogram registration is intractable. However, it should be possible automatically to define corresponding regions in two images, as is done by medical experts.

In this paper, we consider the problem of identifying control points in two images and establishing a correspondence between these points. These points may be used to put a mammogram pair into correspondence, e.g., to establish region correspondence between them. The problem of detecting and matching control points is resolved in two steps. First, each image is analyzed independently to identify potential control points. An intersection of elongated structures is considered to be a potential control point. Next, correspondence between a common subset of potential control points is established by using accumulator matrices and signatures that capture local pattern characteristics. The number of potential matches

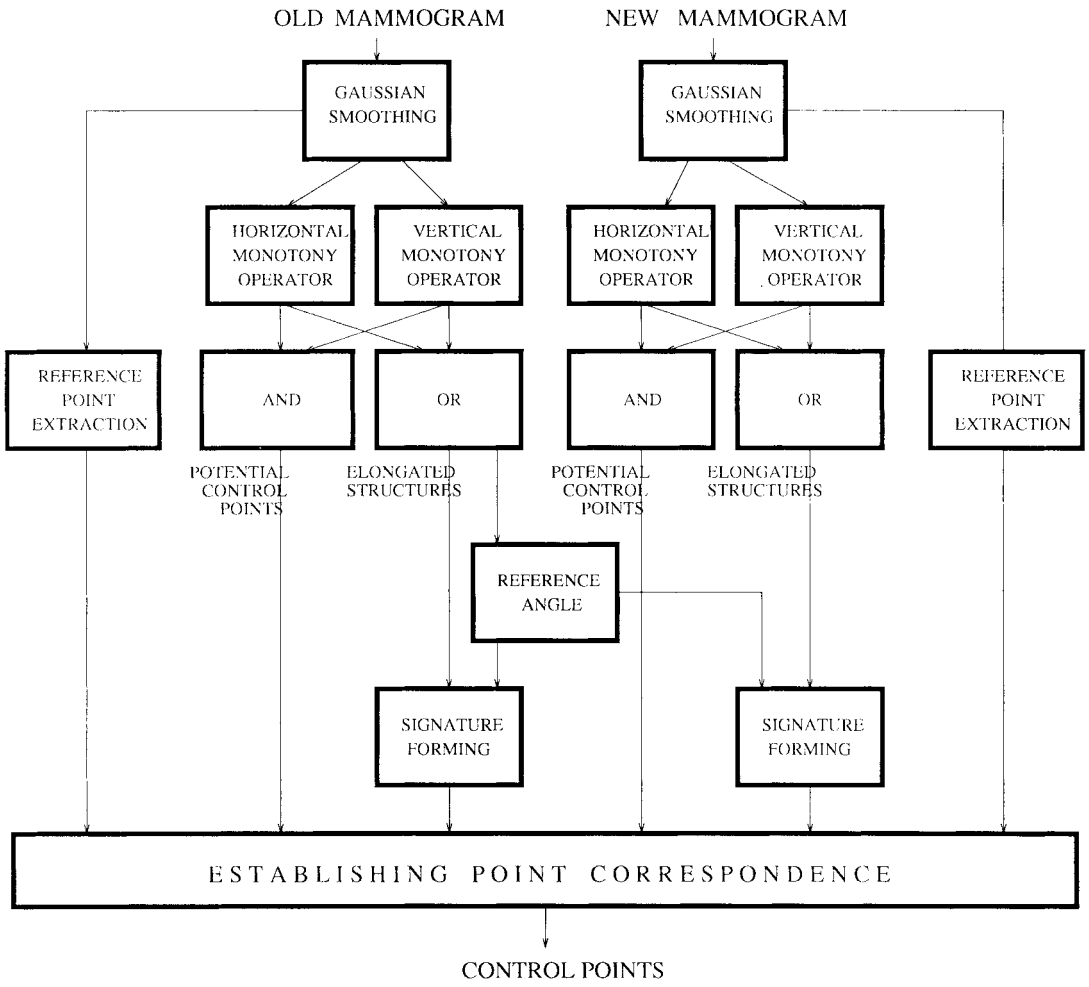

Fig. 1. Processing steps and information flow between processing steps used to identify potential control points and establish their correspondence.

to be considered is reduced by using a pair of reference points that are put into correspondence accurately prior to using accumulator matrices. The reference points may be determined manually or automatically and they may be intrinsic to the breast or defined by external markers during the screening process. The overall procedure for identifying potential control points and establishing correspondence is outlined in Fig. 1. The procedure was applied to 29 pairs of mammograms, and the results were visually evaluated by three observers.

The paper is organized as follows. Section II discusses the problem of automated mammogram followup, and outlines a solution to regional mammogram registration using control points. Section III describes extraction of potential control points, and Section IV summarizes an algorithm establishing correspondence between potential control points. An evaluation of the proposed approach is summarized in Section V.

II. The Problems of Mammogram Followup and Registration

The problem of automatically comparing mammograms acquired at different screenings is very complex because the two images may differ significantly. The primary sources of differences are 1) variations in positioning, 2) variations in compression, and 3) changes normally encountered in breast tissue. The premise behind this work is that there is no rational basis to develop registration techniques that counteract 3-D positioning differences by 2-D image registration (which can be attempted with the techniques of elastic model-based matching [13], [14] or by local point mapping methods [15], [16]). In view of this, we propose surmounting the problem of precise mammogram registration by considering the problem of regional registration instead.

One approach to defining corresponding regions in two mammograms is using control points, i.e., landmark points, and defining regions relative to a set of control points. Considering that the objective of mammogram followup is to compare corresponding regions, in order to reduce the effects of variations in breast tissue density,[1] the regions should be selected such that each region contains primarily a single tissue type. An approach to achieving this goal is utilizing image partitioning and constraining regions to belong to a single partition, as described in [17]. In that work, the geometry

[1]Breast tissue can be classified with respect to radiographic density into radio-opaque (dense tissue appearing as bright uniform regions), radio-lucent (low tissue density and images that show fine detail), and mixed (containing distinct regions corresponding to radio-opaque and to radio-lucent tissue).

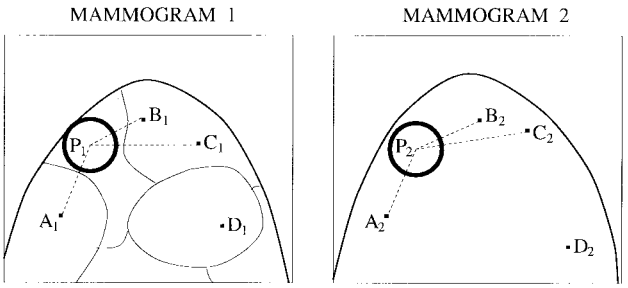

A_i, B_i, C_i, D_i = CONTROL POINTS $i = 1, 2$
P_i = CIRCLE CENTERS $i = 1, 2$
$A_1P_1 \approx A_2P_2$ $B_1P_1 \approx B_2P_2$ $C_1P_1 \approx C_2P_2$

(a)

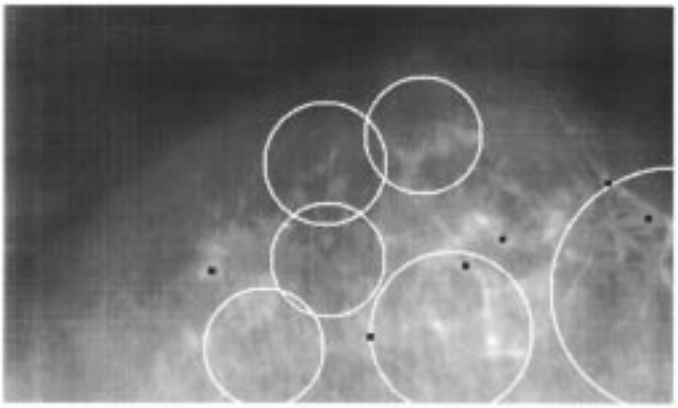

(b)

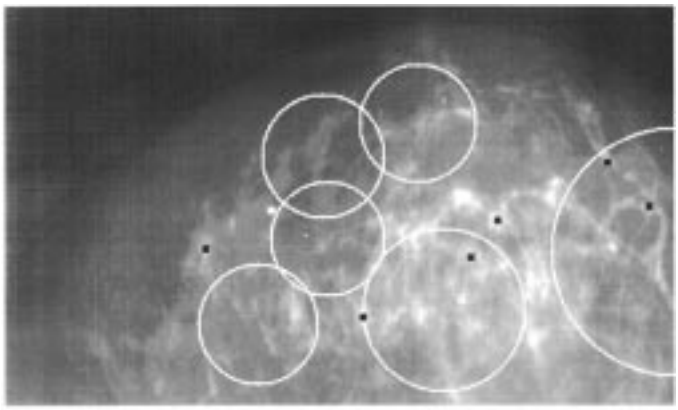

(c)

Fig. 2. Regional correspondence between mammograms. (a) Illustration of procedure, in this case the centers of the regions are determined by distances relative to the three closest control points. (b) Examples of regions determined following this procedure and using control points established using method described in this paper and segmentation of the older mammogram.

of the regions is circular in order to compensate for 2-D rotational distortions arising from digitization. Each circle is defined by the location of its center relative to the control points and its radius, which is determined by segmentation of the older mammogram. The procedure used to define circular regions is illustrated in Fig. 2(a), and examples of the regions obtained are shown in Fig. 2(b). Different procedures may be utilized to determine the centers of the circles, the simplest one assumes that the distances are preserved in two mammograms and determines the centers relative to a subset, e.g., three, of the closest control points as illustrated in Fig. 2(a). More complex procedures take into account elasticity of the tissue and utilize the closest points accordingly. Both mammograms are covered, without gaps, by corresponding overlapping circles. In order to detect abnormalities, regions are compared in terms of their intensity statistics and texture characteristics. Preliminary considerations on region comparison are outlined in [17] and [18].

III. Extraction of Potential Control Points

In this work, we select intersections of prominent elongated structures (such as ducts and blood vessels) as potential control points. The locations of intersections may vary in two images due to positioning differences and compression; however, these variations are minor and the intersections are reliable in establishing regional correspondence.

The intersections between elongated structures are detected by a two-step procedure. In the first step, the mammograms are smoothed (blurred) by Gaussian filtering. In the second step, elongated structures are extracted and intersections are detected by applying modified monotony operators. Blurring reduces the number of potential control points by limiting the analysis to the most prominent structures. Blurring is achieved using three-pass Gaussian filtering. The filter is approximated by a 5×5 kernel and multipass processing, as described in [19]. Typical effects of three-pass smoothing on mammograms are shown by the example in Fig. 3.

Elongated structures are extracted from blurred mammograms by utilizing modified monotony operators. Monotony operators were originally designed to identify points that were used to derive displacement vector fields for image sequences [20]. The monotony operator compares the gray level of an image pixel with that of its eight neighbors and assigns value of zero to eight to it, according to the number of neighbors that have a smaller gray value than the central pixel. Points of interest, such as edges and corners, are determined by selecting pixels that are assigned specific values.

The concept of monotony operator is modified as follows.

- The operator considers two neighborhoods of different size. The geometry of the neighborhood is selected based on processing objectives and may be circular, elliptical, or rectangular.
- The modified monotony operator assigns a value to an image pixel by counting the pixels in the large neighborhood that are related to the pixels in the small neighborhood in a prespecified manner; e.g., it assigns a value to a pixel according to the number of pixels in the large neighborhood that have a higher intensity than the highest intensity in the small neighborhood.
- The output image is binary and is determined by thresholding the output of the monotony operator.

By selecting the geometry of the neighborhood and specifying the relationship between the intensities in the small and large neighborhoods, operators can be designed to detect specific intensity patterns, e.g., elongated structures or intersection points, or perform tasks such as noise removal.

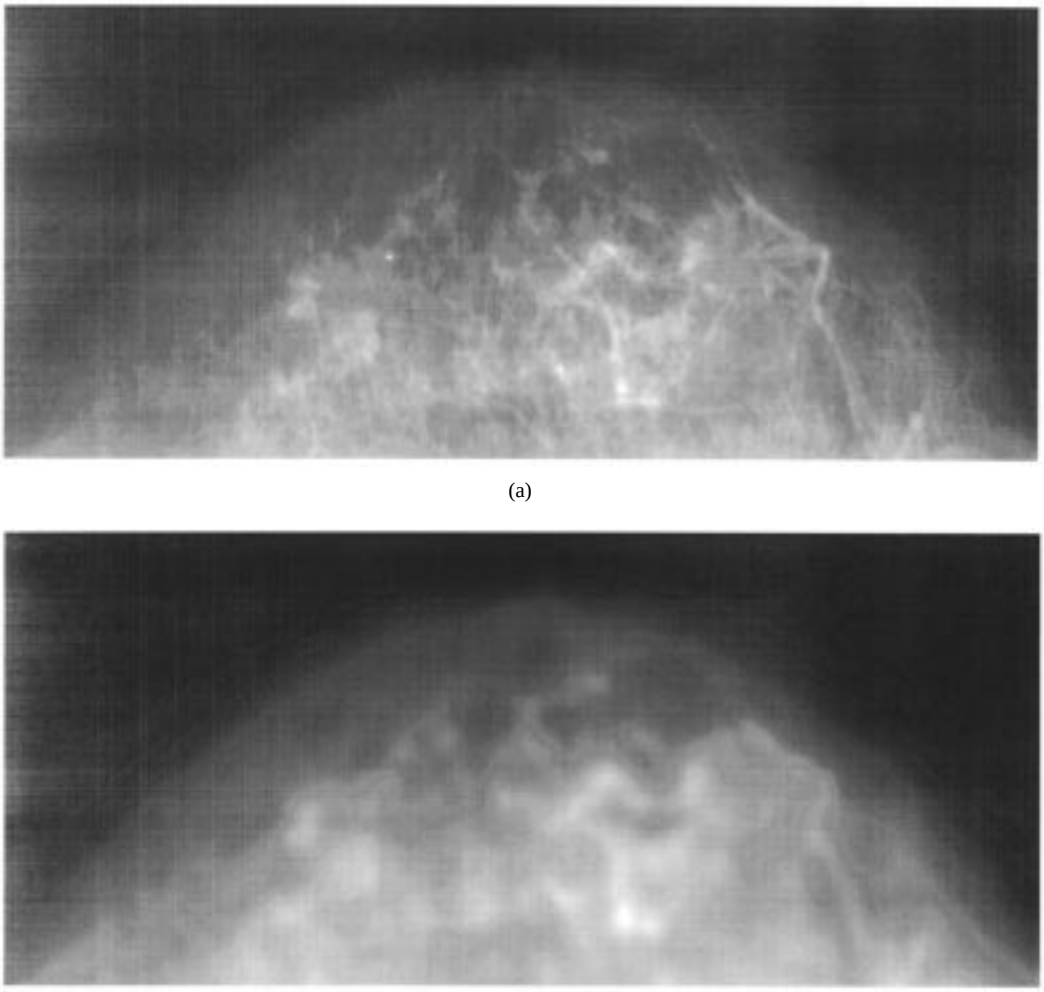

(a)

(b)

Fig. 3. Mammogram smoothing by Gaussian filtering. (a) Original mammogram. (b) Blurred version of the mammogram in (a).

In this work, the operators use narrow rectangular neighborhoods to extract thin, elongated structures (ridges) from blurred mammograms. The original intensity profiles show that ridges are characterized by roof edges that frequently contain superimposed spikes due to noise. The Gaussian operator simplifies the intensity profiles by removing smaller intensity variations and turning the roof edges into flat peaks. Consequently, the objective is to detect the middle point of these flat peaks. For this purpose, the modified monotony operator compares the maximum gray level g_M in the small neighborhood of a pixel (i,j) to gray levels in the large neighborhood of (i,j). If the number of pixels in the large neighborhood that have gray levels higher than g_M exceeds the prespecified threshold T, the pixel (i,j) is labeled one; otherwise, the pixel (i,j) is labeled zero.

The algorithm for the extraction of elongated structures is realized as the following four-step procedure.

- *Step 1: Detection of elongated vertical structures.* A modified monotony operator with $a = \{(k,l)|k = 1, -p \leq l \leq p\}, A = \{(m,n)|m = 1, -q \leq n \leq q\}, q > p$ and threshold[2] $T = (q - p)$ is applied to the blurred mammogram to obtain the binary image with elongated vertical structures [see Fig. 4(a)]. The selection of specific values for p and q is dictated by the mammogram resolution and levels of noise. For mammograms in this work we have used $p = 1$ and $q = 5$. This selection is based on the fact that after smoothing the prominent ridges have a width larger than $11 = (2q + 1)$ pixels. Using a different resolution requires the evaluation of appropriate values for parameters p, q and T based on mammogram characteristics and desired objectives.
- *Step 2: Detection of elongated horizontal structures.* A modified monotony operator with $a = \{(k,l)|-p \leq k \leq p, l = 1\}, A = \{(m,n)|, -q \leq m \leq q, n = 1\}$, and $T = (q - p)$ is applied to the blurred mammogram to obtain the binary image with elongated horizontal structures [see Fig. 4(b)]. Considering that the same resolution was used in both the vertical and horizontal directions, the same values for $p, q,$ and T are used as in Step 1.
- *Step 3: OR-ing of horizontal and vertical images.* A logical OR operation is applied to a pair of horizontal and vertical images in order to obtain an image with elongated

[2]The threshold value ensures that at least 50% of the pixels lying in the larger neighborhood exclusively have intensity higher than the maximum intensity of the small neighborhood.

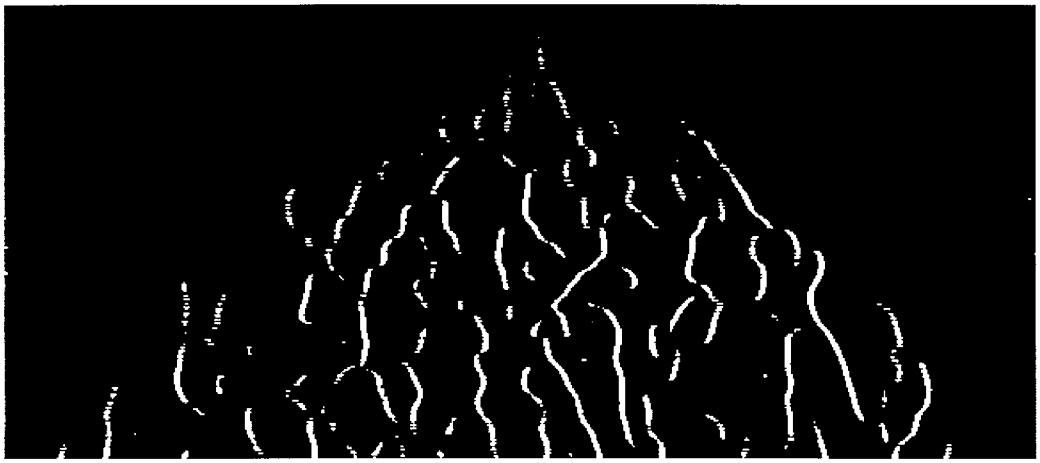

(a)

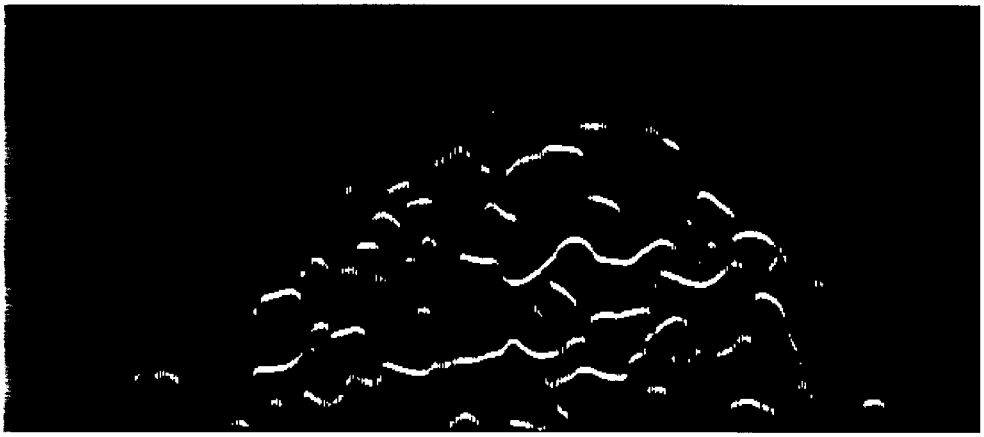

(b)

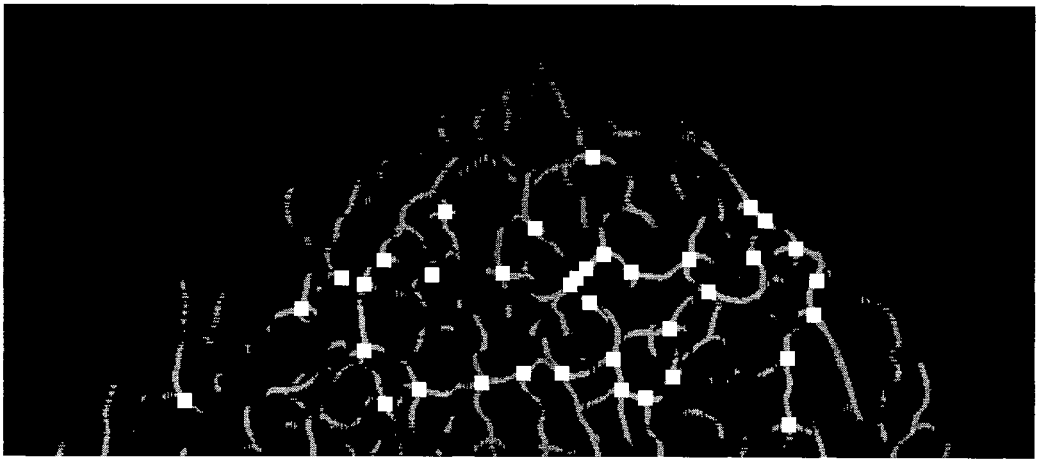

(c)

Fig. 4. Extraction of elongated anatomical structures and detection of potential control points in the image shown in Fig. 3(a). (a) Vertical image. (b) Horizontal image. (c) Image with elongated structures in arbitrary direction with superimposed potential control points.

structures in an arbitrary direction [see Fig. 4(c)]. The binary pattern formed by this operation is used to form signatures when establishing point correspondences (see flowchart in Fig. 1).

- *Step 4: Detection of intersections of elongated structures.* Intersections are obtained by applying a logical *AND* operation to the pair of horizontal and vertical images. The centroids of obtained binary objects constitute the set of potential control points.

An identical procedure is applied to both mammograms. Many of the points detected in one mammogram do not have corresponding points in the other mammogram, as illustrated

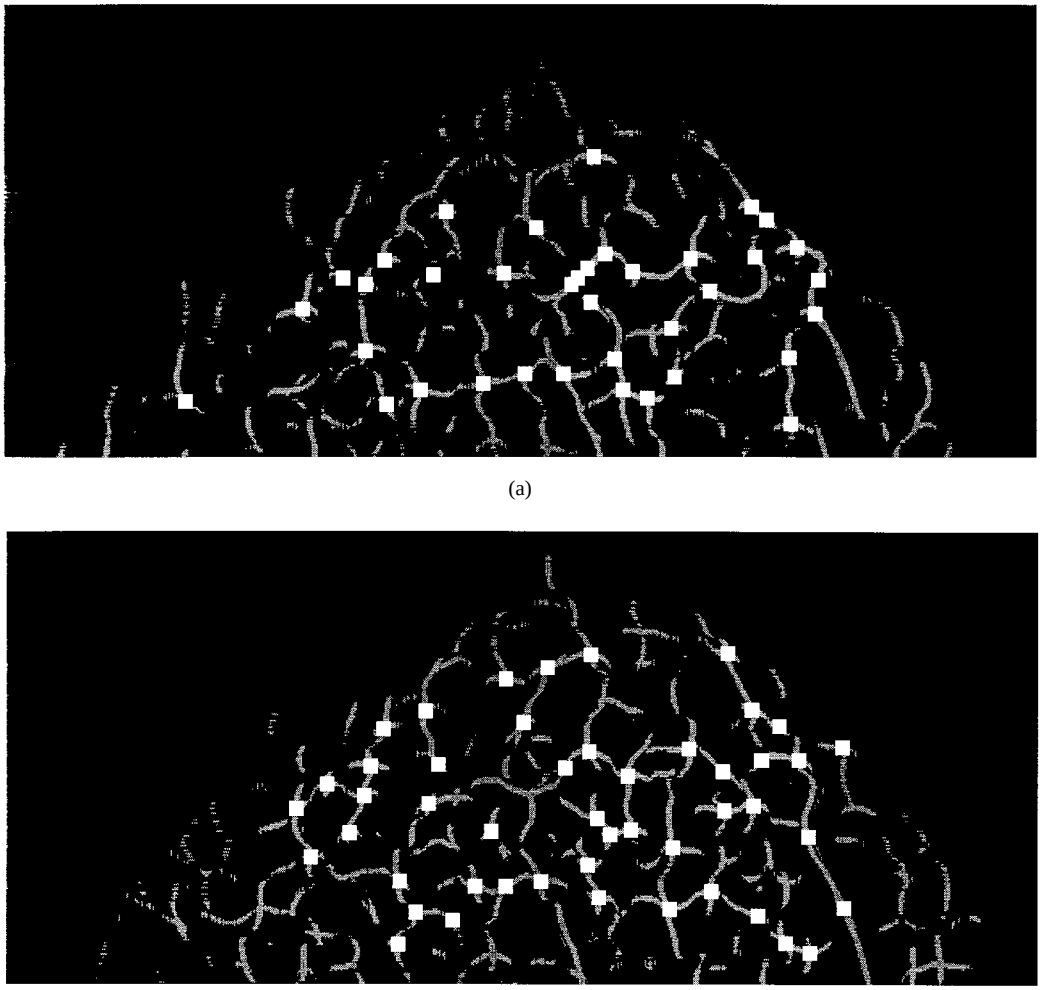

(a)

(b)

Fig. 5. Potential control points extracted from a mammogram pair.

in Fig. 5. The points that they have in common are determined by the algorithm described in Section IV. It is important to note that the procedure for detecting potential control points is applicable to various mammogram types, including those that are predominantly radio-opaque, as is shown by the example in Fig. 6.

IV. Establishing Control Point Correspondence

Given two sets of potential control points, the objective of the correspondence algorithm is to identify the common subset and within it individual point correspondences. This is a point pattern matching problem. The justification of most point pattern matching algorithms includes assumptions about the mapping that relates the two sets of points. Solutions have been proposed to problems involving translation [21], [22], translation combined with rotation [23], general affine transformation [24], and affine transformation combined with random noise [25]. The problem of matching point patterns extracted from mammograms is more difficult because the transformation relating two sets of points cannot be comprehensively modeled. In this work, we propose a solution that uses a pair of reference points combined with local signatures to determine if there is a correspondence between two points. Sections IV-A and IV-B describe the extraction of reference points and signatures, and Section IV-C describes the correspondence algorithm.

A. Identifying Reference Points

The term *reference points* pertains to a pair of points whose correspondence is established accurately in a mammogram pair. The correspondence may be established manually or automatically and may utilize points intrinsic to the breast or defined by external markers used during the screening process. In principle, detection of reference points is independent of detection of potential control points. The reference points are used by the correspondence algorithm to identify possible matches among the two sets of potential control points.

The natural selection, i.e., a point existing in practically every mammogram and independent of viewpoint, is the tip of the nipple, and in the following we describe the procedure used to identify automatically this point in two mammograms. Under normal screening conditions, the tip of the nipple lies approximately on the extrema point of the breast outline. In this work, this point is identified by finding the extrema

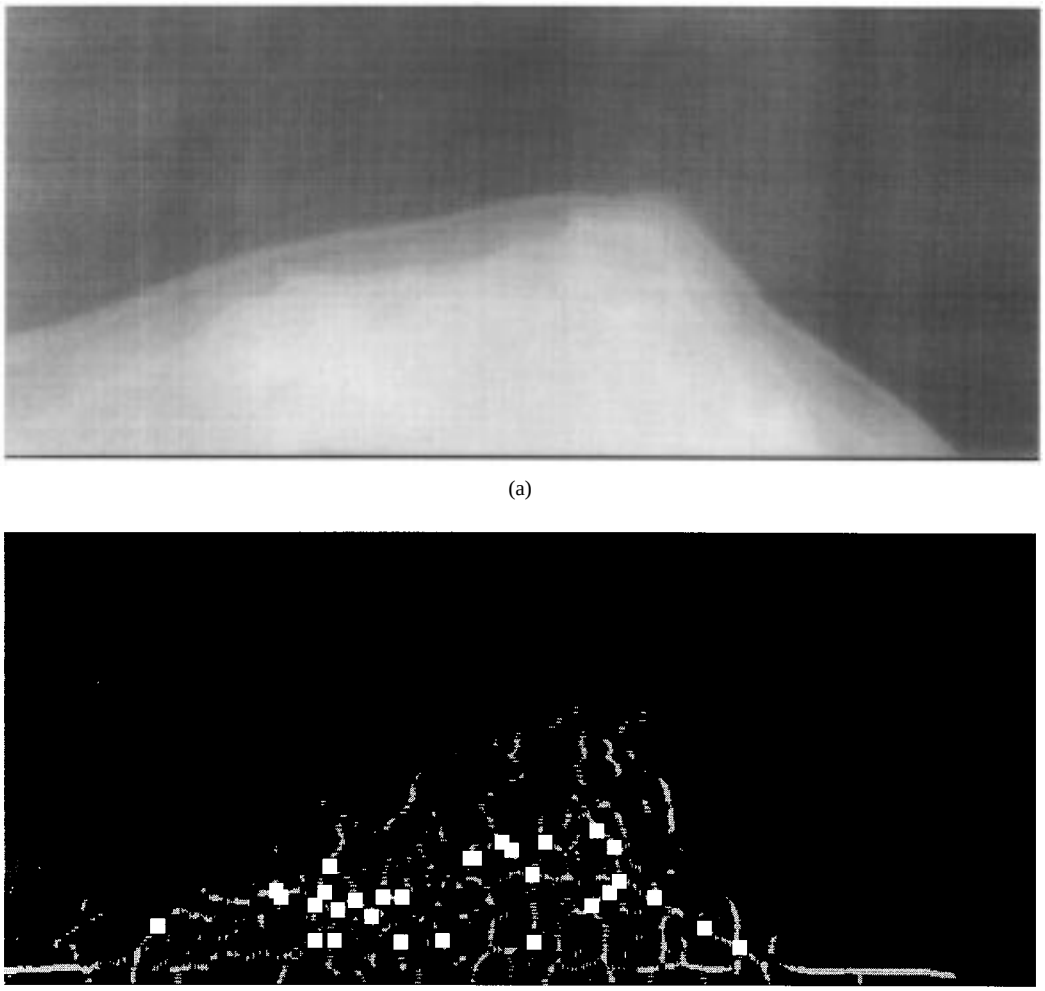

(a)

(b)

Fig. 6. (a) Example of a predominantly radio-opaque mammogram; (b) Elongated anatomical structures with superimposed potential control points extracted from (a).

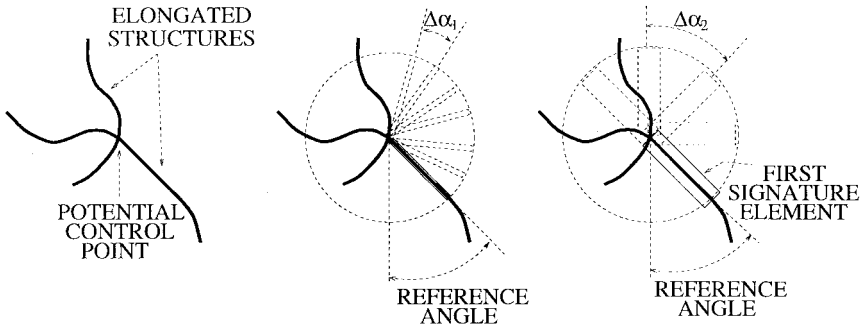

(a) (b) (c)

Fig. 7. Signature forming. (a) Pattern of elongated anatomical structures in the neighborhood of a potential control point. (b) Determination of the reference angle. (c) Determination of signature entries.

of the least mean square error (LMSE) approximation of the breast outline by a quadratic function. The outline is initially determined by the optimum thresholding procedure, [26], applied to the blurred mammograms. The procedure was tested on 29 mammogram pairs, and visually it was confirmed that the reference points were identified consistently. It is pointed out that the same procedure was applied to both the medio-lateral and the cranio-caudal[3] views without adjustments.

[3]The terms *medio-lateral* and *cranio-caudal* refer to routine acquisition positions. In the cranio-caudal projection, compression is applied from the top of the breast with a detector system under the caudal surface. In the medio-lateral projection, compression is applied sidewise from the center of the chest wall toward the outer breast surface.

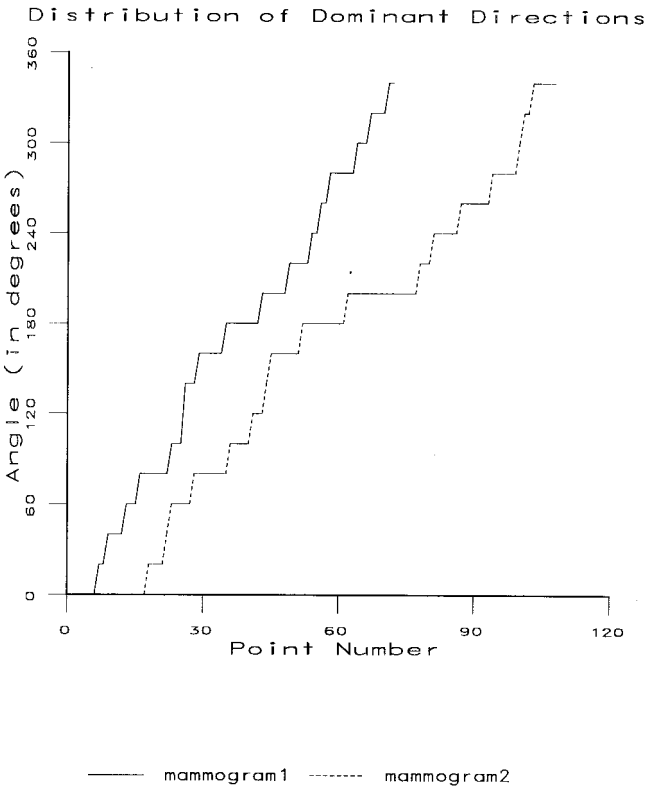

Fig. 8. Distribution of orientations (ordered by angle) of elongated structures at the potential control points in two mammograms from Fig. 3(a).

B. Formations of Signatures and Similarity Criterion

Each potential control point is characterized by a signature that captures the characteristics of the most prominent elongated structure, i.e., the longest of the pair involved in an intersection [see Fig. 7(a)]. The image with elongated anatomical structures is used as an input to signature formation. The procedure consists of the following two steps.

- *Determination of the reference angle.* The reference angle is determined in this implementation by analyzing the older mammogram and identifying the direction of the most prominent elongated structure. This is achieved by examining narrow rectangular neighborhoods oriented in different directions. We use rectangles 20×3 pixels that rotate around a potential control point in steps $\Delta\alpha_1 = 3°$. For each direction the number of nonzero pixels is recorded, and the direction associated with the highest count is selected as the reference angle [see Fig. 7(b)].
- *Forming the signature.* A signature, S, is represented as a vector whose entries are determined by counting the nonzero pixels in a wide rectangle (20×13 pixels) that rotates around a potential control point in steps ($\Delta\alpha_2 = 10°$) starting from the reference angle [see Fig. 7(c)], i.e.,

$$S = [s_1 s_2 \cdots s_{360°/\Delta\alpha_2}]$$

where

$$s_k = \sum_{(i,j)\epsilon A_k} g(i,j), \qquad k = 1, 2, \cdots, \frac{360°}{\Delta\alpha_2}.$$

A_k is the rectangle inclined by $k \times \Delta\alpha_2$ degrees from the reference angle, and $g(i,j)$ is the binary image obtained in Step 3, Section III.

The signatures of two potential control points match if they satisfy the selected similarity criterion. Considering that the two mammograms may be subject to 2-D rotation arising from digitization as well as positioning during acquisition, the elements in one vector may be shifted relative to the elements in the other. The expected rotation is relatively small and we assume less than $\pm 10°$. Consequently, elements in the two signatures may be displaced one position to the right or left. Various similarity criteria may be designed to establish a match between two signatures under these assumptions, e.g., using wavelets [27]. In the present work, we have simplified the criterion to comparing only the first element, s_1^o, in the vector representing a point in the older mammogram and the first, second, and last elements of the vector obtained for a point in the new mammogram, i.e., elements $s_1^n, s_2^n, s_{360°/\Delta\alpha_2}^n$. If for any $s_k^n, k = 1, 2, 360°/\Delta\alpha_2$, both s_1^o and s_k^n are greater than T_1, then there is a match between the two vectors. The specific value for threshold T_1 is dictated by the resolution and level of detail to be detected. For this case study, the elongated structures were on average four pixels wide and thus the 20×13 window oriented in the direction of the structure should ideally capture $20 \times 4 = 80$ pixels belonging to the structure. Assuming that the elongated structure is not perfect, the threshold was selected to be $T_1 = .9 \times 80 = 72$.

The most fundamental issue in using the signatures is verifying that control points are characterized by unique signatures and signatures are preserved in subsequent screenings. Considering that the notions of true and false matches are subjective, and thus it is difficult to verify signature uniqueness by looking at pairs of points, we have studied, instead, the distribution of orientation of elongated structures at the potential control points in mammogram pairs. In all mammogram pairs, the distributions show that there are no preferred orientations, i.e., all orientations are equally likely, and the shape of distribution, i.e., its slope, is preserved in the later mammogram. Fig. 8 shows a typical distribution of orientations (ordered based on angle value) in two mammograms; a steplike appearance of the graphs is due to discretization in the angles when signatures are formed. Experimentation with different signature parameters, including length and width of the rotating rectangle, threshold value and the angle step, has shown that the signature formation is robust and that the distributions do not show significant changes with different parameter selection.

C. Establishing Point Correspondence

The algorithm for establishing point correspondence uses an accumulator matrix (based on work described in [21], [22], and [25]) and signatures to tally votes for a particular match. Given a set of m potential control points in the older mammogram, M_o, and a set of n potential control points in the newer mammogram, M_n, the accumulator matrix is an $m \times n$ array, where an entry $e(p,q)$ corresponds to points labeled p and q in M_o and M_n, respectively. A point

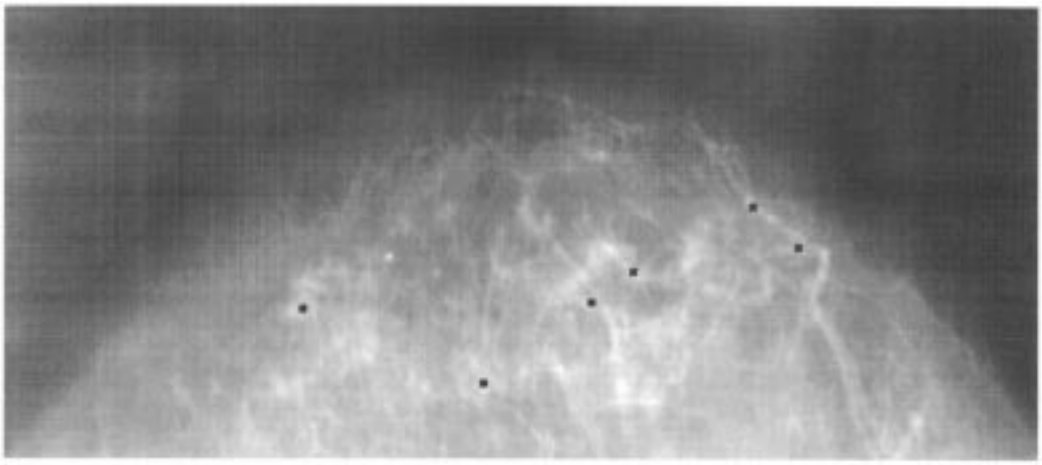

(a)

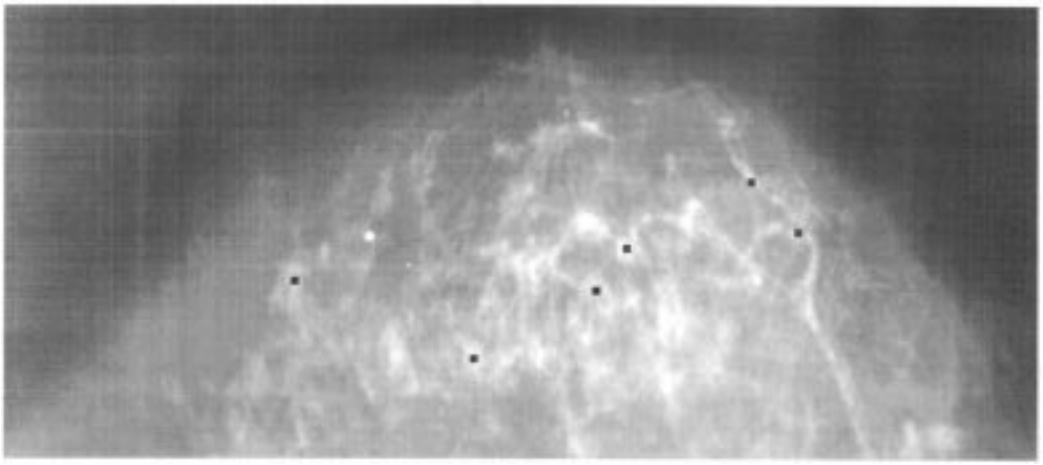

(b)

Fig. 9. Control points extracted from a pair of mammograms superimposed on the original images.

$q(x_q, y_q)$ in M_n is considered to be a possible match of point $p(x_p, y_p)$ in M_o and $e(p, q)$ is incremented if q satisfies the following.

- *Location criterion,* i.e., it lies in the neighborhood $k\times$ l centered at x_c, y_c determined by the intersection[4] of line $y = (y_p - y_o/x_p - x_o)(x - x_n) + y_n$ and circle $(x-x_n)^2+(y-y_n)^2 = (x_o-x_p)^2+(y_p-y_o)^2$. Values k and one are determined by expected differences between the two mammograms and (x_o, y_o) and (x_n, y_n) are the coordinates of the reference points in the old and new mammograms, respectively.
- *Similarity criterion,* i.e., their signatures match in the sense described in Section IV-B

Once a match is established between p and q, for each remaining point in M_o, all points in M_n satisfying location criterion are considered and their signatures are compared. It is noted that a point in M_o may be matched to more than one point in M_n. For each successful match, corresponding entries are updated.

[4]There may exist two points of intersection and the one of interest lies in the area of breast tissue.

The algorithm considers all possible matches between points p and q and then matches all the remaining points. At the end of the voting process the correspondences are determined in the following three steps.

1) Determination of the maximum value in each row and setting to zero the remaining entries in that row
2) Determination of the maximum value within each column as a possible match between a particular pair of points
3) Thresholding the values obtained in Step 2. First, the maximum of all values, $V_{\max}$, is determined and then all entries in the accumulator matrix larger than $.8V_{\max}$ are considered to be the matches

If an insufficient number of matches is established using this procedure, the algorithm is iteratively applied, each time starting with the zero accumulator array, using a progressively larger neighborhood $k\times$ l. In this work we have varied $k\times$ l from 10 $\times$ 10 to 60 $\times$ 60 in steps of ten. We have found neighborhood size 20 $\times$ 20 to be reliable. An example of the established control points for a pair of mammograms is shown in Fig. 9. Six matches were obtained for $k = l = 20$.

TABLE I
RESULT OF VALIDATION WHEN CONSIDERING ONLY "SURE" POINTS. ENTRIES ARE OF THE FORM $P(T)$, WHERE P IS THE PERCENTAGE OF POINTS "IN AGREEMENT" AND T IS THE NUMBER OF POINTS CONSIDERED. THE TOTAL NUMBER OF POINTS IS 122

	algorithm	radiologist	observer 1	observer 2
algorithm	-	91 (103)	71 (77)	75 (85)
radiologist	-	-	83 (66)	82 (76)
observer 1	-	-	-	78 (63)

TABLE II
RESULT OF VALIDATION WHEN CONSIDERING BOTH "SURE" AND "NOT SURE" POINTS. ENTRIES ARE OF THE FORM $P(T)$, WHERE P IS THE PERCENTAGE OF POINTS "IN AGREEMENT" AND T IS THE NUMBER OF POINTS CONSIDERED. THE TOTAL NUMBER OF POINTS IS 122

	algorithm	radiologist	observer 1	observer 2
algorithm	-	86 (109)	72 (99)	69 (106)
radiologist	-	-	78 (91)	77 (99)
observer 1	-	-	-	67 (91)

V. RESULT EVALUATION

The algorithm for control point extraction was tested on 29 mammogram pairs acquired in the time span of six months to two years. The spatial resolution of digitized mammograms varied from 0.1 to 0.5 mm. Based on tissue characteristics, 16 pairs have predominantly radio-lucent characteristics and the remaining 13 pairs contain mixed tissue types. Using the algorithm described in Section III, an average of 70 potential control points was detected per mammogram. Using the algorithm described in Section IV-C, with a neighborhood size 20×20 and a threshold $n/2$, where n is the total number of potential control points in the new mammogram, an average of five correspondences was established per mammogram pair. Since there is no precise knowledge on the location of control points, the algorithm performance was validated by visual inspection. The validation was performed independently by three observers (who had no knowledge about the algorithm), an experienced radiologist, and two casual observers.

A. Organization of the Validation Expeiment

The validation experiment was conducted as follows. Each observer was shown a mammogram pair, where the older mammogram contained highlighted points selected by the algorithm. The observers were then asked to identify the corresponding points in the newer mammogram and were also asked to assign a "level of confidence" to the established matches. Namely, if a match was established with a high degree of certainty, the confidence level was "sure"; if a match was determined with a lower degree of certainty, the confidence level was "not sure"; in the case when no match could be assigned, a point was labeled "don't know." No time limit was imposed upon the observers during the validation experiment. The observers were trained and encouraged to use enhancement techniques in the experiment (e.g., histogram equalization).

TABLE III
RESULT OF VALIDATION WHEN CONSIDERING "SURE" POINTS ONLY: ENTRIES ARE COMPUTED USING (5)

	algorithm	radiologist	observer 1	observer 2
algorithm	-	77	45	52
radiologist	-	-	45	51
observer 1	-	-	-	40

TABLE IV
RESULT OF VALIDATION WHEN CONSIDERING BOTH "SURE" AND "NOT SURE" POINTS: ENTRIES ARE COMPUTED USING (5)

	algorithm	radiologist	observer 1	observer 2
algorithm	-	77	58	60
radiologist	-	-	58	63
observer 1	-	-	-	50

TABLE V
RESULT OF VALIDATION WHEN CONSIDERING ONLY "SURE" POINTS AND "EASY" MAMMOGRAMS. ENTRIES WERE GENERATED USING (5)

	algorithm	radiologist	observer 1	observer 2
algorithm	-	81	48	57
radiologist	-	-	49	53
observer 1	-	-	-	37

TABLE VI
RESULT OF VALIDATION WHEN CONSIDERING BOTH "SURE" AND "NOT SURE" POINTS AND "EASY" MAMMOGRAMS: ENTRIES WERE GENERATED USING (5)

	algorithm	radiologist	observer 1	observer 2
algorithm	-	81	53	64
radiologist	-	-	56	66
observer 1	-	-	-	46

B. Evaluation of the Algorithm Performance

The evaluation procedure compared the points obtained by the algorithm with the points identified by the observers. Based on the spatial resolution, the algorithm and an observer were considered to be in agreement if the distance between the two points was less than 10 pixels. Table I summarizes the validation results when only points labeled "sure" were considered. Each entry in the table is of the form $P(T)$, where P is the percentage of points "in agreement" and T is the number of points considered. For example, the entry (*algorithm, radiologist*) $=$ 91 (103) indicates that 91% of 103 "sure" control points determined by the radiologist are "in agreement" with corresponding points determined by the computer. Table II includes both "sure" and "not sure" points.

Tables III and IV show the normalized form of the same results. The entries in these tables were calculated using

$$\text{agreement} = \text{percentage} \times \frac{\text{number of points considered}}{\text{total number of points}} \tag{1}$$

where *percentage* represents the percentage of points "in agreement." From Tables I–IV, it follows that the agreement between the radiologist and the algorithm is significantly higher than the agreement between the casual observers and the algorithm. It is pointed out that the potential control points are not points that are naturally selected by a radiologist when examining the mammograms. The average distance between the points determined by the radiologist and the computer was 9 pixels, and the average distance between the casual observers and the computer was 14 pixels. Assuming the worst case, i.e., spatial resolution of 0.5 mm, the actual average distance was 4.5 mm and 7 mm, respectively.

In order to test the sensitivity of the algorithm to breast tissue characteristics, results pertaining to 16 pairs of mammograms exhibiting a high degree of radio-lucency were analyzed separately. Such mammograms are generally labeled "easy" to read. The validation results on this subset are shown in Tables V and VI. These tables indicate that the conclusions drawn for the whole set of mammograms remain valid for this subset, thus showing that the algorithm performance does not depend on mammogram characteristics.

VI. Conclusions

This paper describes part of an effort to build a system for automated mammogram analysis using mammogram followup. Mammograms of the same patient acquired at different times are compared in order to detect changes indicative of cancer. The paper concentrates on the problem of determining unique feature points in two mammograms and establishing their correspondence. These points can be further used to establish regional correspondence and, thus, to surmount difficulties related to precise registration by a more feasible problem of regional registration. The control points are detected using the modified monotony operator and matched using accumulator matrix and signatures.

The proposed procedure was validated by visual inspection of 29 mammogram pairs, and a high degree of agreement was found between the observers and the algorithm, and in particular between the radiologist and the algorithm. The analysis of results relative to breast tissue characteristics revealed that the algorithm performs equally well on different tissue types. In the next stage of research, we plan to evaluate the usefulness of established correspondences in detecting changes due to cancer.

Acknowledgment

The mammograms were supplied by St. Luke's Hospital, Bethlehem, PA.

References

[1] B. D. Stewart *et al.*,"Computer image processing in mammographic screening: A review," *Automedica*, vol. 15, pp. 23–45, 1992.

[2] A. P. Dhawan, Buelloni, and R. Gordon, "Enhancement of mammographic features by optimal adaptive neighborhood image processing," *IEEE Trans. Med. Imag.*, vol. MI-5, pp. 8–15, 1986.

[3] P. G. Tahoces *et al.*, "Enhancement of chest and breast radiographs by automatic spatial filtering," *IEEE Trans. Med. Imag.*, vol. 10, pp. 330–335, 1991.

[4] S. Astley and P. Miller, "Automated detection of breast asymmetry using anatomical features," in *State of the Art in Digital Mammographic Image Analysis*, K. W. Bowyer and S. Astley, Eds. Singapore: World Scientific, 1994.

[5] W. P. Kegelmeyer Jr., "Evaluation of stellate lesion detection in standard mammogram data set," *Int. J. Pattern Recognit. Artif. Intell.*, vol. 7, pp. 1477–1492, Dec. 1993.

[6] F. Winsberg, *et al.*, "Detection of radiographic abnormalities in mammography by means of optical scanning and computer analysis," *Radiology*, vol. 89, pp. 211–216, 1967.

[7] H. D. Li, M. Kallergi, L. P. Clarke, and V. K. Jain, "Markov random field for tumor detection in digital mammography," *IEEE Trans. Med. Imag.*, vol. MI-14, pp. 565–576, 1995.

[8] C. B. Cadwell *et al.*, "Characterization of mammographic perenchymal pattern by fractal dimension," *SPIE Med. Imag. III: Image Process.*, vol. 1092, pp. 10–16, 1989.

[9] R. M. Nishikawa *et al.*, "Computer-aided detection and diagnosis of masses and clustered microcalcifications from digital mammograms," in *State of the Art in Digital Mammographic Image Analysis*, K. W. Bowyer and S. Astley, Eds. Singapore: World Scientific, 1994.

[10] H. Barman, G. Granlund, and L. Haglund, "Feature extraction for computer-aided analysis of mammograms," in *State of the Art in Digital Mammographic Image Analysis*, K.W. Bowyer and S. Astley, Eds. Singapore: World Scientific, 1994.

[11] Y. Chitre, A.P. Dhawan, and M. Moskowitz, "Artificial neural network based classification of mammographic microcalcifications using image structure features," in *State of the Art in Digital Mammographic Image Analysis*, K.W. Bowyer and S. Astley, Eds. Singapore: World Scientific, 1994.

[12] Liang Shen, R. M. Rangayyan, and J. E. Leo Desautels, "Detection and classification of mammographic calcifications," in *State of the Art in Digital Mammographic Image Analysis*, K. W. Bowyer and S. Astley, Eds. Singapore: World Scientific, 1994.

[13] R. Bajscy and S. Kovacic, "Multiresolution elastic matching," *Comput. Vis., Graph., Image Process.*, vol. 46, pp. 1–21, 1989.

[14] D. J. Burr, "A dynamical model for image registration," *Comput. Graph. Image Processing*, vol. 15, pp. 102–112, 1981.

[15] J. Flusser, "An adaptive method for image registration," *Pattern Recognit.*, vol. 25, pp. 45–54, 1992.

[16] A. Goshtasby, "Image registration by local registration," *Image Vis. Computing*, vol. 6, pp. 255–261, 1988.

[17] N. Vujovic, P. Bakic, and D. Brzakovic, "Detection of potentially cancerous signs by mammogram followup," in *Proc. 3rd Int. Workshop on Digital Mammography*, Chicago, IL, 1996.

[18] D. Brzakovic *et al.*, "Mammogram analysis by comparison with previous screenings," in *Proc. 2nd Int. Workshop on Digital Mammography*, York, U.K., 1994.

[19] P. J. Burt, "Fast filter transforms for image processing," *Comput. Graph. Image Process.*, vol. 16, pp. 20–51, 1981.

[20] R. Kories and G. Zimmerman, "A versatile method for the estimation of displacement vector fields from image sequences," in *Proc. Workshop on Motion: Representation and Analysis*, 1986.

[21] D. J. Kahl, A. Rosenfeld, and A. Danker, "Some experiments in point pattern matching," *IEEE Trans. Syst., Man, Cybern.*, vol. SMC-10, pp. 105–116, 1980.

[22] S. Ranade and A. Rosenfeld, "Point pattern matching by relaxation," *Pattern Recognit.*, vol. 12, pp. 269–275, 1980.

[23] D. Brzakovic and N. Vujovic, "Authentication of random patterns by finding a match in an image database," *Image Vis. Comput.*, no. 14, pp. 485–499, 1996.

[24] Y. Lamdan and H. J. Wolfson, "Geometric hashing: a general and efficient model-based recognition scheme," in *Proc. ICCV, IEEE*, 1988.

[25] D. Skea, I. Barrodale, R. Kuwahara, and R. Poeckert, "A control point matching algorithm," *Pattern Recognit.*, vol. 26, pp. 269–276, 1993.

[26] N. Otsu, "A threshold selection method from gray-level histograms," *IEEE Trans. Syst., Man, Cybern.*, vol. SMC-9, pp. 62–66, 1979.

[27] H. Sari-Sarraf and D. Brzakovic, "1-D signal classification by multiscale wavelet representation," in *Proc. SPIE Int. Symp. Optical Engineering in Aerospace Sensing*, Orlando, FL, 1992.

Nenad Vujovic (SM'95) received the B.Sc. in electrical engineering from the University of Belgrade, Belgrade, Yugoslavia, in 1991, where he specialized in the area of telecommunications. He received the M.S. degree in electrical engineering in 1992 from the University of Tennessee, Knoxville. He is currently a Ph.D. student in the Department of Electrical Engineering and Computer Science at Lehigh University, Bethlehem, PA.

His research interests are image processing and pattern recognition.

Dragana Brzakovic (M'81) received the B.Sc. in electrical engineering from the University of Belgrade, Belgrade, Yugoslavia, in 1976, and the M.E. and Ph.D. degrees in electrical engineering in 1979 and 1984, respectively, from the University of Florida, Gainesville.

From 1984 to 1992, she was with the Department of Electrical and Computer Engineering, University of Tennessee, Knoxville. Since September 1992, she has been an Associate Professor in the Department of Electrical Engineering and Computer Science, Lehigh University, Bethlehem, PA, where she is teaching courses in pattern recognition, image processing, and computer vision. Her current research interests include the areas of image understanding, knowledge-based pattern recognition, and applied artificial intelligence, specializing in texture analysis.